Ann Med Res

Current issue list available at Ann Med Res

Annals of Medical Research

journal page: annalsmedres.org

Morton's neuroma or its mimics: Diagnostic yield of magnetic resonance imaging and radiographic markers in patients referred with a clinical suspicion

Gizem Timocin Yigman [a,*], Hande Ozen Atalay [a]

[a]*Koç University, Faculty of Medicine, Department of Radiology, Istanbul, Türkiye*
**Corresponding author: gizemtimocin1@gmail.com (Gizem Timocin Yigman)*

MAIN POINTS

- Only two-thirds of patients referred with a clinical suspicion of Morton's neuroma were confirmed to have the diagnosis on magnetic resonance imaging.
- Bursitis was the most frequent alternative diagnosis, highlighting its importance as the main differential diagnosis for MN.
- The 3/4 interphalangeal angle was significantly greater in patients with Morton's neuroma and showed diagnostic value, whereas other angular parameters were not discriminatory.
- The Vulcan sign is a specific radiographic marker for Morton neuroma but not for bursitis.
- To the best of our knowledge, this is the first study conducted exclusively in patients referred with a clinical suspicion of Morton neuroma, addressing diagnostic overlap in this unique population.

Cite this article as: Timocin Yigman G, Ozen Atalay H. Morton's neuroma or its mimics: Diagnostic yield of magnetic resonance imaging and radiographic markers in patients referred with a clinical suspicion. *Ann Med Res*. 2026;33(2):79–85. doi: 10.5455/annalsmedres.2025.09.283.

ABSTRACT

Aim: To determine the prevalence of Morton's neuroma (MN) among patients referred with a clinical suspicion of MN, identify alternative diagnoses, and assess whether angular measurements and the Vulcan sign may help differentiate.

Materials and Methods: This retrospective study included 265 feet from 244 patients (mean age, 50.7±13.0 years; 75% female) referred for magnetic resonance imaging with a presumptive diagnosis of MN between January 2020 and June 2025. All patients underwent radiography and magnetic resonance imaging. Morphometric parameters, including the hallux valgus angle, intermetatarsal angle, and interphalangeal angle (IPA), were measured according to the affected web space (2/3 or 3/4). The Vulcan sign was documented on radiographs. Statistical comparisons were performed using the Mann–Whitney U, chi-square, and Fisher's exact tests.

Results: MN was diagnosed in 167 feet (63.0%), while alternative diagnoses were in 98 (37.0%). Bursitis (32.8%), hallux valgus (30.9%), adventitial bursitis (24.5%), hallux rigidus (12.5%), and stress reaction (8.3%) were the most frequent mimics. The 3/4 IPA was significantly greater in MN than in non-MN feet ($p<0.001$).ROC analysis confirmed limited discriminatory performance, with the 3/4 IPA achieving an AUC of 0.60. Comparisons between bursitis and non-bursitis groups revealed no significant differences in any angular parameters. The Vulcan sign was significantly associated with MN in both the 2nd ($p=0.006$) and 3rd ($p<0.001$) web spaces, but no discriminatory value was found for bursitis. Its diagnostic performance was higher in the third web space (AUC 0.62) than in the second (AUC 0.51).

Conclusion: This is the first study conducted exclusively in patients referred with a clinical suspicion of MN. The 3/4 IPA demonstrated a modest yet significant association with MN, while the Vulcan sign showed relative specificity for MN compared with bursitis. These results underscore the importance of detailed assessment in clinical practice to differentiate MN from its mimics.

Keywords: Morton's neuroma, Metatarsalgia, Magnetic resonance imaging, Radiography, Diagnostic imaging, Bursitis

Received: Oct 02, 2025 **Accepted:** Dec 01, 2025 **Available Online:** Feb 25, 2026

INTRODUCTION

Metatarsalgia is defined as forefoot pain localized to the metatarsal region. A common clinical problem with a broad spectrum of potential causes. Morton's neuroma (MN) is one of the most common and well-recognized Histologically, MN does not represent a true neuroma but rather a neuro–bursal complex characterized by perineural fibrosis, axonal degeneration, and vascular proliferation [1, 2]. It typically occurs in the third intermetatarsal space, less commonly in the second, and has a marked female predominance [3, 4].

MN clinically presents with burning plantar pain, tingling or numbness of the toes, and the classic sensation of "walking on a pebble." Symptoms usually worsen with weight bearing and the use of constrictive footwear [5]. Examination find-

ings, such as Mulder's sign or palpation-induced pain in the web space, may raise suspicion, but they are not sufficiently specific to confirm the diagnosis [4]. Therefore, imaging plays a pivotal role. Ultrasound (US) is an easily accessible and dynamic modality with high sensitivity and specificity [1, 6], whereas magnetic resonance imaging (MRI) is the gold standard because of its soft tissue contrast and ability to characterize other findings [4, 7].

The differential diagnosis of MN is broad and includes intermetatarsal bursitis, plantar plate tears, metatarsophalangeal synovitis, submetatarsal bursitis (adventitious bursitis), stress fractures, tendon sheath tumors, and hallux valgus or rigidus [1, 2, 8]. These diagnoses may present similar symptoms and complicate diagnostic accuracy. In particular, intermetatarsal bursitis can easily mimic MN both clinically and radiologically and cause difficulty in accurate diagnosis [1]. In addition, forefoot static disorders, such as hallux valgus and hallux rigidus, are frequent contributors to metatarsalgia and may co-exist with MN [7, 9].

Differentiating MN from its mimics is challenging in clinical practice. Most patients referred with a preliminary diagnosis of MN have alternative pathologies, particularly bursitis [2]. Previous studies have attempted to define distinguishing imaging or clinical features to separate MN from other etiologies; however, diagnostic overlap persists [4]. Importantly, morphologic parameters have been studied in the context of forefoot disorders. To our knowledge, no previous study has specifically investigated a cohort consisting exclusively of patients referred with a clinical suspicion of MN. It is essential to systematically evaluate imaging-confirmed diagnoses and explore whether specific radiographic and MRI-based morphologic features can distinguish MN from its mimics to clarify the true prevalence of MN among such clinically suspected cases.

The aim of this study, which represents the first to focus exclusively on patients referred with a clinical suspicion of MN, is therefore to determine the proportion of patients referred with a clinical suspicion of MN who actually demonstrate MN or alternative diagnoses, to investigate whether IMA and IPA differ between patients with MN and those with other diagnoses or normal findings, and to evaluate the association between the Vulcan sign on radiographs and the presence of MN.

MATERIALS AND METHODS

This retrospective study was conducted in accordance with the principles of the Declaration of Helsinki and was approved by our institutional Biomedical Research Ethics Committee (Koç University Ethics Committee, Approval number: 2025.388.IRB2.175). All patients provided written informed consent before radiological evaluation, including permission for anonymized use of data for research purposes.

Study participants

We retrospectively reviewed patients referred with a clinical suspicion of MN who underwent both radiography and MRI of the foot between January 2020 and June 2025 at our tertiary care institution. The inclusion criterion was referral for forefoot pain with "MN?" as the clinical query. We excluded patients with prior foot surgery, known traumatic foot injuries, congenital anomalies, or examinations with nondiagnostic image quality.

Imaging protocol

All patients initially underwent radiography in standard anteroposterior and oblique projections, followed by MRI examinations using a dedicated coil and 1.5T or 3T scanners (MAGNETOM Aera and Skyra, Siemens Healthcare, Erlangen, Germany). Was examined in the supine position with the foot in neutral alignment and padded to minimize motion. Our institutional routine foot MRI protocol included coronal T1-weighted spin-echo images (TR/TE, 675/27 ms; FoV, 165×110 mm; slice thickness, 3.3 mm; acquisition matrix, 960×800); axial T1-weighted spin-echo images (TR/TE, 735/28 ms; FoV, 120×120 mm; slice thickness, 3.6 mm; acquisition matrix, 614×768); coronal proton density fat-suppressed fast spin-echo (PD-FS TSE) (TR/TE, 3250/40 ms; FoV, 165×110 mm; slice thickness, 3.0 mm; acquisition matrix, 806×768); axial PD-FS TSE (TR/TE, 4820/45 ms; FoV, 109×120 mm; slice thickness, 3.6 mm; acquisition matrix, 512×704); sagittal T1-weighted turbo inversion recovery magnitude (TIRM, fat-suppressed) images (TR/TE, 4500/28 ms; FoV, 247×180 mm; slice thickness, 3.3 mm; acquisition matrix, 352×320). Intravenous contrast was not administered in any case as per the departmental protocol for suspected MN.

Image analysis

All radiographs and magnetic resonance images were independently reviewed by two radiologists with more than 10 and 5 years of experience, respectively. MN was diagnosed when a fusiform lesion of low-to-intermediate signal on T1- and T2-weighted sequences was identified in the intermetatarsal space, typically contiguous with the plantar digital nerve. A fluid-signal lesion within the intermetatarsal bursa was defined as bursitis. Additional forefoot pathologies were systematically assessed. Hallux valgus was diagnosed on radiographs with a hallux valgus angle of >15°. Hallux rigidus was identified in the presence of joint space narrowing, osteophyte formation, and subchondral sclerosis of the first metatarsophalangeal joint and diagnosed based on both radiographs and magnetic resonance imaging. On MRI, adventitial bursitis was accepted as a fluid-signal lesion adjacent to the medial eminence of the first metatarsal head. Stress reaction was diagnosed based on marrow edema-like signal intensity on T2-weighted images without a distinct fracture line. Morphometric measurements included the HVA, IMA, and

https://doi.org/10.5455/annalsmedres.2025.09.283

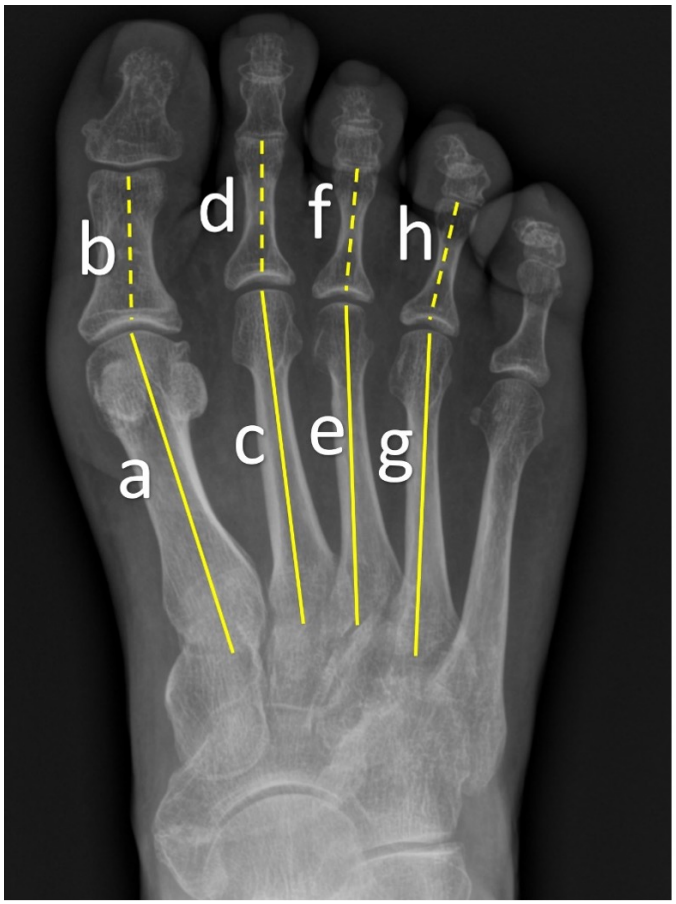

Figure 1. Measurement of angular parameters on dorsoplantar radiographs The hallux valgus angle was defined as the angle between line a (first metatarsal axis) and line b (proximal phalanx of the hallux). The 2/3 IMA was measured between lines c and e, whereas the 3/4 IMA was measured between lines e and g. The 2/3 IPA was measured between lines d and f, and the 3/4 IPA was measured between lines f and h.

IPA at the 2/3 or 3/4 interspaces depending on the pathology site. For patients with MN or bursitis in both the second and third interspaces, both corresponding angles were measured (Figure 1). On plain radiographs, the presence or absence of the Vulcan sign, which is characterized by the presence of a V-shaped appearance in the interphalangeal space, was documented at the 2/3 and 3/4 phalanx interspaces.

Statistical analysis

All statistical analyses were performed using the Statistical Package for the Social Sciences (version 28.0; IBM Corp., Armonk, NY, USA). Continuous variables, including IMA and IPA, are presented as medians with interquartile ranges. The corresponding 2/3 or 3/4 IPA and IMA were compared with those without MN in the same interspace using the Mann–Whitney U test. Separate analyses were also conducted to compare MN and bursitis cases. Patients showing both conditions in the same web space were excluded, and bursitis-positive versus bursitis-negative groups were evaluated accordingly. The presence of the Vulcan sign on radiographs was analyzed in relation to MN and bursitis within the 2nd and 3rd interspaces using Fisher's exact test or chi-square test

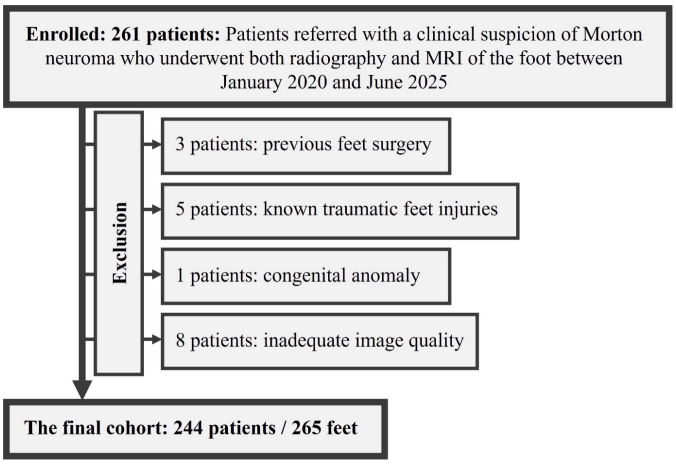

Figure 2. Flowchart of the study design.

as appropriate. In addition, ROC curve analyses were performed to assess the diagnostic performance of the 2/3 and 3/4 IPA and IMA values as well as the Vulcan sign. The area under the curve (AUC), optimal cutoff, sensitivity, and specificity were calculated for each parameter. A p-value of < 0.05 was considered statistically significant. Effect size analyses were also performed to assess the magnitude of significant associations: for Mann–Whitney U tests, the effect size ($r = Z/\sqrt{N}$) was calculated, and for categorical comparisons, Cramer's V was used. The intraclass correlation coefficient (ICC) was used to assess the interobserver reproducibility of angular measurements, and agreement for the Vulcan sign was evaluated with Cohen's kappa coefficient. A p-value of < 0.05 was considered statistically significant.

RESULTS

A total of 261 patients were initially evaluated. Of these, 3 patients were excluded due to previous foot surgery, 5 patients due to known traumatic foot injuries, and 1 patient due to congenital anomaly and 8 patients due to inadequate images for evaluation. The final cohort comprised 265 feet from 244 patients, including 21 patients with bilateral examinations (Figure 2). The mean age was 50.7±13.0 years, and 199 (75%) were female, while 66 (25%) were male.

On MRI, 167 feet (63.0%) demonstrated MN, while 98 (37.0%) did not. In our cohort, alternative diagnoses included bursitis in 87 feet (32.8%), hallux valgus in 82 (30.9%), adventitial bursitis in 65 (24.5%), hallux rigidus in 33 (12.5%), and stress reaction in 22 (8.3%) (Table 1). Multiple diagnoses were identified in 144 patients. The distribution of MN was as follows: 46 (17.4%) in web space 2, 102 (38.5%) in web space 3, and 19 (7.2%) involving both interspaces. Bursitis was observed in web space 2 in 20 cases (7.5%), in web space 3 in 24 cases (9.1%), and in both interspaces in 43 cases (16.2%). The Vulcan sign on radiographs was present in 126 patients (47.5%). Patients with MN were slightly older than those without MN (mean 52.3±12.8 vs. 48.1±13.2 years, $p<0.005$), whereas gender distribution did not differ signifi-

https://doi.org/10.5455/annalsmedres.2025.09.283

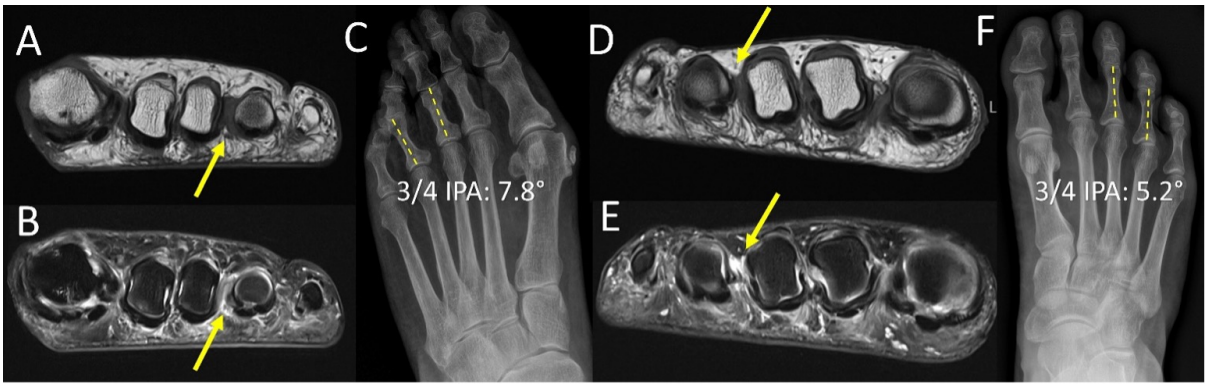

Figure 3. Comparison of the interphalangeal angle (IPA) in Morton neuroma (MN) and bursitis (A–C) A 71-year-old woman with MN in the third web space. Coronal T1-weighted (A) and fat-suppressed T2-weighted (B) magnetic resonance images show a fusiform lesion (arrows). The corresponding radiograph (C) demonstrates a 3/4 IPA of 7.8°, which is enlarged compared with non-MN cases. A 56-year-old female patient with intermetatarsal bursitis in the third web space. Coronal T1-weighted (D) and fat-suppressed T2-weighted (E) magnetic resonance images showing a fluid-signal lesion within the intermetatarsal bursa (arrows). The corresponding radiograph (F) shows a 3/4 IPA of 5.2°.

Table 1. Demographic and clinical characteristics of the study population.

Characteristic		
Total number of patients per foot		244/265
Age, mean ± SD (years)		50.7±13.0
Sex, n (%)	Female	199 (75%)
	Male	66 (25%)
Morton neuroma and its differential diagnoses	Morton neuroma, n (%)	167 (63.0%)
	Bursitis, n (%)	87 (32.8%)
	Hallux valgus, n (%)	82 (30.9%)
	Adventitial bursitis, n (%)	65 (24.5%)
	Hallux rigidus, n (%)	33 (12.5%)
	The stress reaction, n (%)	22 (8.3%)
	Multiple diagnoses (n)	144

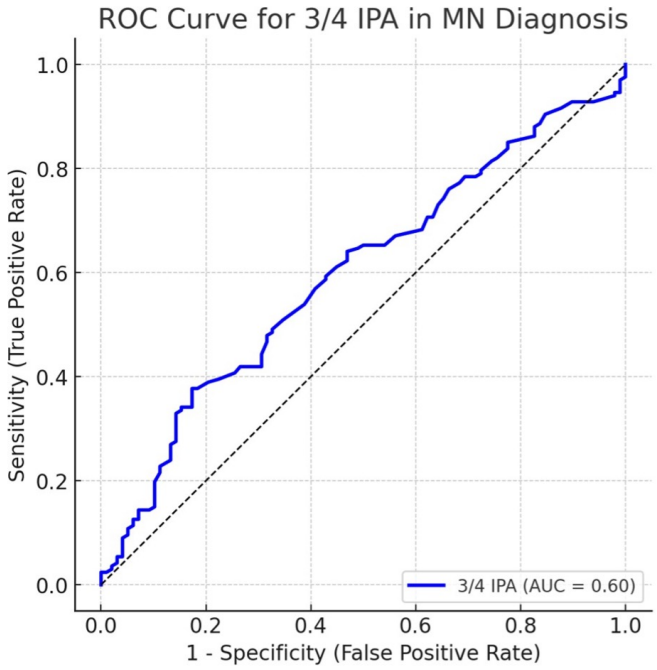

Figure 4. ROC curve of the 3/4 IPA for MN diagnosis.

Table 2. Comparison of interphalangeal angle (IPA) and intermetatarsal angle (IMA) between the Morton neuroma and non-Morton neuroma groups.

Angle	MN (median, range)	Non-MN (median, range)	p-value
2/3 IPA	4.3° (0.7–17.2)	4.2° (0.4–19.8)	= 0.96
2/3 IMA	3.2° (0.8–7.9)	3.0° (0.6–10.0)	= 0.94
3/4 IPA	5.1° (0.3–13.7)	3.6° (0.3–14.2)	< 0.001
3/4 IMA	5.2° (0.9–11.7)	4.4° (0.8–11.9)	= 0.056

IPA: interphalangeal angle; IMA: intermetatarsal angle; MN: Morton neuroma; CI, confidence interval.

Table 3. Comparison of the angles between the Bursitis and Non-Bursitis groups.

Angle	Bursitis (median, range)	Non-Bursitis (median, range)	p-value
2/3 IPA	3.4° (0.8–8.6)	4.3° (0.4–19.8)	= 0.22
2/3 IMA	2.3° (0.6–5.4)	3.1° (0.7–10.0)	= 0.056
3/4 IPA	4.0° (0.4–9.3)	4.4° (0.3–14.2)	= 0.22
3/4 IMA	5.5° (0.8–9.5)	4.5° (0.9–11.9)	= 0.27

IPA: interphalangeal angle; IMA: intermetatarsal angle.

https://doi.org/10.5455/annalsmedres.2025.09.283

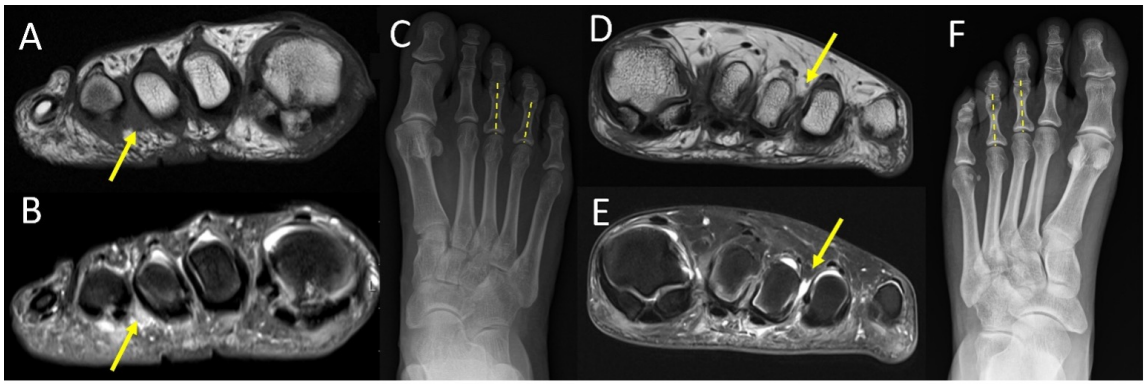

Figure 5. Comparison of the Vulcan sign in MN and bursitis. A–C. A 48-year-old woman with MN in the third web space. Coronal T1-weighted (A) and fat-suppressed T2-weighted (B) magnetic resonance images show a fusiform lesion (arrows). The corresponding radiograph (C) demonstrates a positive Vulcan sign at the 3/4 interspace. A 53-year-old female patient with intermetatarsal bursitis in the third web space. Coronal T1-weighted (D) and fat-suppressed T2-weighted (E) magnetic resonance images showing a fluid-signal lesion within the intermetatarsal bursa (arrows). The corresponding radiograph (F) shows the absence of the Vulcan sign.

Table 4. Association between the Vulcan Sign and Morton neuroma and bursitis.

Group	Web space	V-sign (+)	V-sign (--)	p-value
MN vs. Non-MN	2nd	24.6%	10.1%	= 0.006
MN vs. Non-MN	3rd	56.0%	22.3%	< 0.001
Bursitis vs. non-bursitis	2nd	10.0%	13.6%	= 1.0
Bursitis vs. non-bursitis	3rd	33.3%	40.7%	= 0.657

MN: Morton neuroma; V-sign: Vulcan sign.

Table 5. ROC analysis of interphalangeal angle and Vulcan sign.

Parameter	AUC (95% CI)	Cut-off	Sensitivity (%)	Specificity (%)
3/4 IPA	0.60 (0.53--0.66)	5.8°	37	82
V-sign (3rd web)	0.62 (0.56--0.68)	Presence	45	77
V-sign (2nd web)	0.51 (0.47--0.55)	Presence	24.6	89.9

IPA: interphalangeal angle; V-sign: Vulcan sign; AUC: Area under the curve.

cantly between the groups (p>0.005). For MN in the 2nd web space, the median 2/3 IPA was 4.3° (range, 0.7–17.2) compared with 4.2° (0.4–19.8) in non-MN feet. The corresponding IMA measured 3.2° (0.8–7.9) versus 3.0° (0.6–10.0). For MN in the third web space, the median 3/4 IPA was 5.1° (0.3–13.7) compared with 3.6° (0.3–14.2) in non-MN feet. The 3/4 IMA was 5.2° (0.9–11.7) in MN cases versus 4.4° (0.8–11.9) in non-MN cases (Table 2). For bursitis in the 2nd web space, the median 2/3 IPA was 3.4° (0.8–8.6) versus 4.3° (0.4–19.8) in non-bursitis cases, whereas the IMA was 2.3° (0.6–5.4) versus 3.1° (0.7–10.0). For bursitis in the 3rd web space, the median 3/4 IPA was 4.0° (0.4–9.3) compared with 4.4° (0.3–14.2) in non-bursitis feet, and the intermetatarsal angle was 5.5° (0.8–9.5) compared with 4.5° (0.9–11.9) (Table 3).

For MN located in the 2nd web space, neither the 2/3 IMA nor the IPA significantly differed between MN-positive and MN-negative feet (p=0.96 and p=0.94, respectively). In contrast, for MN located in the 3rd web space, the 3/4 IPA was significantly greater in MN-positive feet than in MN-negative feet (p<0.001), whereas the IMA did not differ significantly (p=0.056) (Figure 3). In addition, ROC analysis demonstrated that the 3/4 IPA achieved an AUC of 0.60 (95% CI, 0.53–0.66) with a cutoff of 5.8°, yielding 37% sensitivity and 82% specificity (Figure 4). The corresponding effect size for the 3/4 IPA was r = 0.28, indicating a small-to-moderate association between increased angle and MN.

Comparisons between bursitis and nonbursitis cases revealed no significant differences in either web space. For the 2nd web space bursitis, no significant difference was observed in both the 2/3 IPA (p=0.22) and the IMA (p=0.056) compared with the non-bursitis group, although the latter displayed a borderline trend toward higher values in bursitis cases. For the 3rd web space bursitis, neither the 3/4 IPA (p=0.22) nor the IMA (p=0.27) significantly differed between bursitis and nonbursitis feet (Figure 5).

The Vulcan sign was significantly associated with the presence of MN in the 2nd (24.6% vs. 10.1%, p=0.006) and 3rd (56.0% vs. 22.3%, p<0.001) web spaces. However, no significant association was observed between the Vulcan sign and bursitis in either the 2nd (10.0% vs. 13.6%, p=1.0) or 3rd (33.3% vs.

https://doi.org/10.5455/annalsmedres.2025.09.283

40.7%, p=0.657) web spaces (Table 4; Figure 4). In addition, the Vulcan sign achieved the highest AUC of 0.62 (95% CI 0.56–0.68), sensitivity of 45%, and specificity of 77% compared to the 2nd web space AUC of 0.51 (95% CI 0.47–0.55) (Table 5). The effect size analysis showed a small association in the 2nd web space (Cramer's V=0.17) and a moderate association in the 3rd web space (Cramer's V=0.34), supporting the stronger relationship between the Vulcan sign and MN at the 3rd interspace.

A second musculoskeletal radiologist independently repeated all angular measurements in a subset of patients to assess measurement reproducibility. The interobserver agreement was excellent, with the ICC values ranging from 0.87 to 0.94 (p<0.001). Interobserver agreement for the Vulcan sign was substantial, with $\varkappa = 0.77$ (p<0.001).

DISCUSSION

To our knowledge, this is the first study conducted in a cohort of patients referred with a clinical suspicion of MN. We demonstrated that only 63% of feet have an MN on MRI. Bursitis is the most common of the alternative diagnoses encountered, followed by hallux valgus, adventitial bursitis, hallux rigidus, and stress reaction. With respect to morphometric analyses, the 3/4 IPA was significantly greater in patients with MN than in those without, while no significant differences were observed in the 2/3 IPA or IMA measurements. In contrast, comparisons between bursitis, which is the main differential diagnosis, and non-bursitis did not yield significant differences in terms of angles. Finally, the Vulcan sign was strongly associated with MN compared with the non-MN patient group in both the 2nd and 3rd web spaces, whereas no association was observed with bursitis compared with the non-bursitis group.

Consistent with our findings, Zaleski et al evaluated 45 patients with MN and demonstrated that the 3/4 IPA was significantly increased compared with controls, with good diagnostic performance. They also reported a modest increase in the 3/4 IMA, albeit with lower specificity [10]. In contrast, we analyzed a much larger cohort of 265 feet from 244 patients in our study, and beyond confirming the diagnostic value of the 3/4 IPA, our results extend these observations by demonstrating its utility in differentiating MN from normal feet and other differential diagnoses, particularly bursitis. In contrast, two earlier studies failed to identify significant differences in IMA or IPA between MN and controls. Both studies were limited by smaller sample sizes (84 and 100 patients, respectively) and primarily focused on comparisons with controls [11, 12]. The larger sample size and unique referral-based cohort in our study likely increased the sensitivity for detecting subtle morphometric differences, particularly in the 3/4 IPA.

Galley et al evaluated 100 MN patients and 100 controls and reported that the sign had high specificity but limited sensitivity for distinguishing MN [13]. In our study, which included a larger cohort of 244 patients, a significant association was found between the Vulcan sign and MN in both the 2nd and 3rd web spaces. Importantly, we extended these observations by specifically testing its performance against bursitis, the main differential diagnosis, and demonstrated that the Vulcan sign does not discriminate between bursitis and non-bursitis cases. This consistency reinforces its role as a specific, although not sensitive, marker for MN and highlights its lack of value in separating MN from bursitis.

Finally, Togei et al approached angular measurements from a different perspective, comparing patients with and without metatarsalgia irrespective of the underlying diagnosis. They found significant differences in HVA and IMA, which were interpreted as indicators of dynamic instability rather than diagnostic indicators [14]. In contrast, our study specifically targeted a referral-based MN cohort and demonstrated the diagnostic implications of angular measurements and radiographic signs within this clinical context. From a clinical perspective, these findings suggest that simple radiographic assessment for the Vulcan sign may aid in raising suspicion for MN in patients presenting with metatarsalgia, particularly in settings where magnetic resonance imaging is not readily available. In addition, measuring the 3/4 IPA on standard imaging could provide supportive diagnostic information when interpreted alongside MRI findings, potentially improving diagnostic confidence in distinguishing MN from its mimics.

Limitations

This study has several limitations. First, the retrospective design of the study causes a potential risk of selection bias. Second, although our patient cohort is larger than those of previous studies, a larger cohort with prospective evaluation is still required. Third, clinical correlations such as pain severity, symptom duration, and functional scores were not included due to the radiological aspect of the study. Finally, although bilateral examinations were performed in 21 patients, each foot was analyzed as an independent observation because most displayed different pathologies or angular measurements between sides. Given the known asymmetry in foot morphology and deformities, such as hallux valgus, this approach was considered appropriate; however, the potential for partial interfoot dependency remains a minor limitation. In addition, although some parameters showed statistically significant associations with MN, their diagnostic performance metrics were modest, indicating limited clinical applicability when interpreted in isolation.

CONCLUSION

In conclusion, our study was conducted in the largest cohort and the first study to include patients specifically referred with a clinical suspicion of MN. It was demonstrated that nearly one-third of our cohort had alternative diagnoses rather than MN. Among the morphometric parameters, only the 3/4 IPA showed a significant association with MN at the 3rd web space,

https://doi.org/10.5455/annalsmedres.2025.09.283

whereas bursitis or other diagnoses showed no significant relationship. The Vulcan sign has emerged as a useful radiographic marker for MN but not for bursitis. These findings highlight the importance of detailed imaging evaluation in patients with metatarsalgia due to diagnostic overlap between MN and its mimics and suggest that in routine radiological evaluation for MN, IPA measurement and Vulcan sign may be helpful for correct diagnosis.

Ethics Committee Approval: This retrospective study was conducted in accordance with the Declaration of Helsinki and approved by the Biomedical Research Ethics Committee of Koc University with a reference number of 2025.388.IRB2.175 (Date: 12.09.2025).

Informed Consent: The study had retrospective design, no additional procedures were performed. Informed consent forms are obtained from each patient before the radiological examination in our institution as a clinical routine.

Peer-review: Externally peer-reviewed.

Conflict of Interest: The authors declared no potential conflicts of interest with respect to the research, authorship, and/or publication of this article.

Author Contributions: GTY: Conceptualization; Data curation; Investigation; Methodology; Project administration; Supervision; Writing–review and editing. HOA: Methodology; Formal analysis; Writing–original draft; Software.

Financial Disclosure: The authors received no financial support for the research, authorship, and/or publication of this article.

Artificial Intelligence Disclosure: AI-assisted tool (ChatGPT-5.2) was used solely for language editing.The authors are fully responsible for the content of article.

REFERENCES

1. Son HM, Chai JW, Kim YH A problem-based approach in musculoskeletal ultrasonography: central metatarsalgia. *Ultrasonography.* 2022;41(2):225-242. doi: 10.14366/usg.21193.
2. Ganguly A, Warner J, Aniq H. Central Metatarsalgia and Walking on Pebbles: Beyond Morton Neuroma. *AJR Am J Roentgenol.* 2018;210(4):821-833. doi: 10.2214/AJR.17.18460.
3. Bencardino J, Rosenberg ZS, Beltran J, Liu X, Marty-Delfaut E. Morton's neuroma: is it always symptomatic? *AJR Am J Roentgenol.* 2000;175(3):649-653. doi: 10.2214/ajr.175.3.1750649.
4. Santiago FR, Muñoz PT, Pryest P, Martínez AM, Olleta, N.P. Role of imaging methods in diagnosis and treatment of Morton's neuroma. *World J Radiol.* 2018;10(9):91-99. doi: 10.4329/wjr.v10.i9.91.
5. Jain S, Mannan K. The diagnosis and management of Morton's neuroma: a literature review. *Foot Ankle Spec.* 2013;6(4):307-317. doi: 10.1177/1938640013493464.
6. Xu Z, Duan X, Yu X, Wang H, Dong X, Xiang Z. The accuracy of ultrasonography and magnetic resonance imaging for the diagnosis of Morton's neuroma: a systematic review. *Clin Radiol.* 2015;70(4):351-8. doi: 10.1016/j.crad.2014.10.017.
7. Palka O, Guillin R, Lecigne R, Combes D. Radiological approach to metatarsalgia in current practice: an educational review. *Insights Imaging.* 2025;16(1):94. doi: 10.1186/s13244-025-01945-3.
8. Reijnierse M, Griffith JF. High-resolution ultrasound and MRI in the evaluation of the forefoot and midfoot. *J Ultrason.* 2023;23(95):e251-e271. doi: 10.15557/jou.2023.0033.
9. Coughlin MJ, Shurnas PS. Hallux rigidus: demographics, etiology, and radiographic assessment. *Foot Ankle Int.* 2003;24(10):731-743. doi: 10.1177/107110070302401002.
10. Zaleski M, Tondelli T, Hodel S, Rigling D, Wirth S. The interphalangeal angle as a novel radiological measurement tool for Morton's neuroma - a matched case-control study. *J Foot Ankle Res.* 2021;14(1):62. doi: 10.1186/s13047-021-00502-7.
11. Park YH, Jeong SM, Choi GW, Kim HJ. The role of the width of the forefoot in the development of Morton's neuroma. *Bone Joint J.* 2017;99-B(3):365-368. doi: 10.1302/0301-620X.99B3.BJJ-2016-0661.R1.
12. Naraghi R, Bremner A, Slack-Smith L, Bryant A. Radiographic Analysis of Feet With and Without Morton's Neuroma. *Foot Ankle Int.* 2017;38(3):310-317. doi: 10.1177/1071100716674998.
13. Galley J, Sutter R, Germann C, Pfirrmann CWA. The Vulcan salute sign: a non-sensitive but specific sign for Morton's neuroma on radiographs. *Skeletal Radiol.* 2022;51(3):581-586. doi: 10.1007/s00256-021-03851-3.
14. Togei K, Shima H, Hirai Y et al. Relationship Between the Relative Length of the Second Metatarsal and Occurrence of Metatarsalgia in Patients With Hallux Valgus. *Foot Ankle Int.* 2025;46(2):217-226. doi: 10.1177/10711007241298682.

https://doi.org/10.5455/annalsmedres.2025.09.283